

Electronic Supplementary Information for

Ultra-stretchable Ion Gels Based on Physically Cross-linked Polymer Networks

Zhehao Tang,^{†[a](#)} Dong Liu,^{†[a](#)} Xiaolin Lyu,^{*[b](#)} Yadi Liu,^a Yun Liu,^a Weilu Yang,^a Zhihao Shen^{*[a](#)} and Xinghe Fan^{*[a](#)}

^a Beijing National Laboratory for Molecular Sciences, Key Laboratory of Polymer Chemistry and Physics of Ministry of Education, Center for Soft Matter Science and Engineering, and College of Chemistry and Molecular Engineering, Peking University, Beijing, 100871, China

^b Key Laboratory of Advanced Materials Technologies, College of Materials Science and Engineering, Fuzhou University, Fuzhou, 350108, China

Table of Contents

Table S1. Feed ratio of P(EA- <i>co</i> -AA)	S2
Table S2. Sample composition and tensile properties of ion gels	S2
Table S3. Parameters for the VTF fitting of the conductivity data	S2
Scheme S1. Chemcial structure of [EMIM][TFSI]	S3
Figure S1. GPC curves of P(EA- <i>co</i> -AA)	S3
Figure S2. ¹ H NMR spectra of P(EA- <i>co</i> -AA)	S3
Figure S3. DSC thermograms of P(EA- <i>co</i> -AA) with different ratios	S4
Figure S4. Photographs of the ion gel before and after stretching	S4
Figure S5. Storage and loss moduli of the ion gel from sample 78-16-6	S4
Figure S6. FTIR and WAXS results of PEA- <i>co</i> -AA and 78-0-22	S5
Figure S7. Tensile properties of ion gels reported in recent years	S5
Figure S8. TGA thermogtam of the ion gel	S5
Figure S9. DSC thermogram of the ion gel	S6
Figure S10. DSC thermogram of the ion gel	S6
Figure S11. Sensing performance of the ion gel	S6
Figure S12. Schematic illustration of the preparation of the ion gel	S7
References	S7

Table S1. Feed ratio of P(EA-*co*-AA).

Sample	AIBN (mg)	EA (g)	AA (g)	Dioxane (mL)
P(EA- <i>co</i> -AA)-1	10.0	5.25	0.540	12
P(EA- <i>co</i> -AA)-2	10.0	5.00	0.720	12
P(EA- <i>co</i> -AA)-3	10.0	4.50	1.08	12
P(EA- <i>co</i> -AA)-4	10.0	4.00	1.44	12
P(EA- <i>co</i> -AA)-5	10.0	3.00	2.16	12
P(EA- <i>co</i> -AA)-6	10.0	2.00	2.88	12

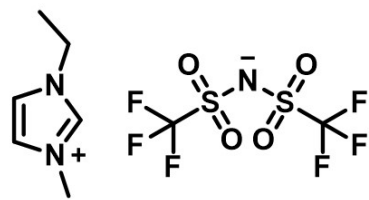
Table S2. Sample composition and tensile properties of different P(EA-*co*-AA-*co*-AANa) ion gels.

Sample ^{a)}	Polymer ^{b)}	NaOH (mg)	EA (mol%)	AA (mol%)	AANa (mol%)	Stress (kPa)	Strain (%)
78-22-0	P(EA- <i>co</i> -AA)-3	0.00	78	22	0	-	-
78-19-3	P(EA- <i>co</i> -AA)-3	5.00	78	19	3	-	-
78-16-6	P(EA- <i>co</i> -AA)-3	10.0	78	16	6	60	> 6500
78-10-12	P(EA- <i>co</i> -AA)-3	20.0	78	10	12	980	2600
78-5-17	P(EA- <i>co</i> -AA)-3	30.0	78	5	17	1100	790
78-0-22	P(EA- <i>co</i> -AA)-3	40.0	78	0	22	1270	470
88-0-12	P(EA- <i>co</i> -AA)-1	20.0	88	0	12	180	2700
85-3-12	P(EA- <i>co</i> -AA)-2	20.0	85	3	12	740	2500
70-18-12	P(EA- <i>co</i> -AA)-4	20.0	70	18	12	2600	910
52-36-12	P(EA- <i>co</i> -AA)-5	20.0	52	36	12	-	-
38-50-12	P(EA- <i>co</i> -AA)-6	20.0	38	50	12	-	-

^{a)} Named based on the mole percentages of the three monomers, ^{b)} 400 mg of polymer in each sample.

Table S3. Parameters for the VTF fitting of the conductivity data

σ_0 (S cm ⁻¹)	E_a (kJ mol ⁻¹)	T_0 (K)
0.086	2.04	157



Scheme S1. Chemical structure of [EMIM][TFSI].

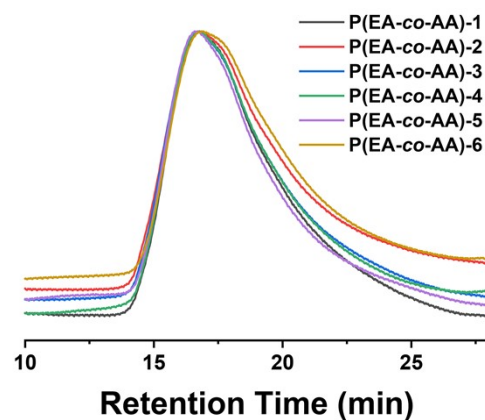


Figure S1. GPC curves of P(EA-*co*-AA).

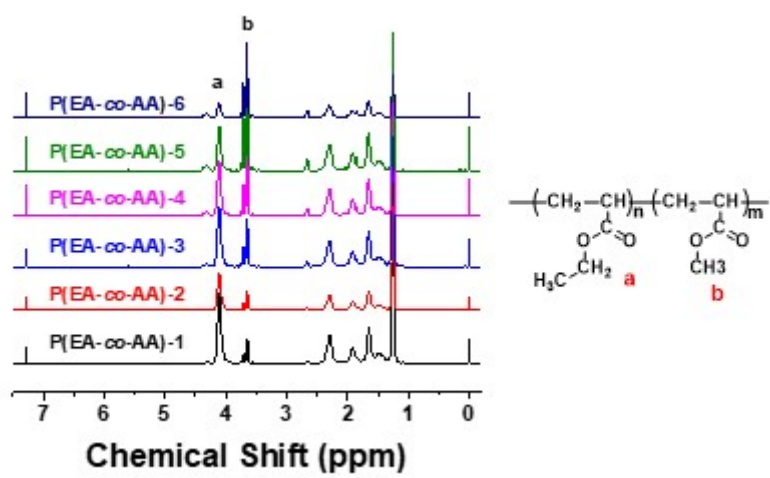


Figure S2. ¹H NMR spectra of P(EA-*co*-AA) samples with CDCl₃ as the solvent.

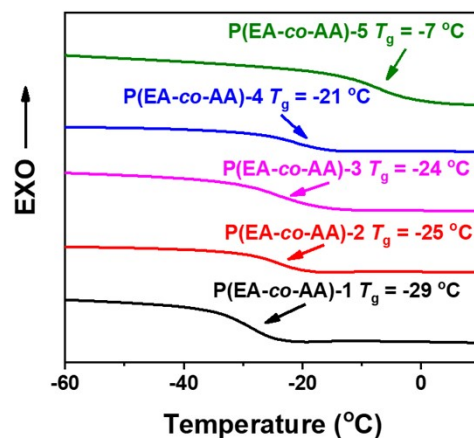


Figure S3. DSC thermograms of P(EA-*co*-AA) with different EA/AA ratios.

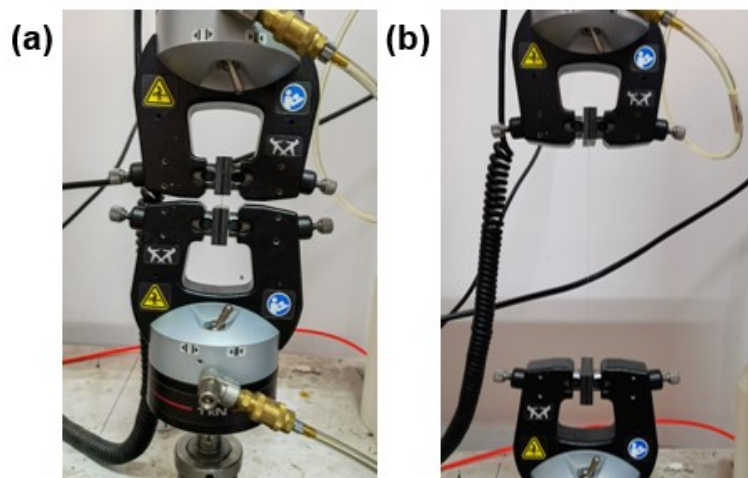


Figure S4. Photographs of the P(EA-*co*-AA-*co*-AANa) ion gel before (a) and after (b) stretching.

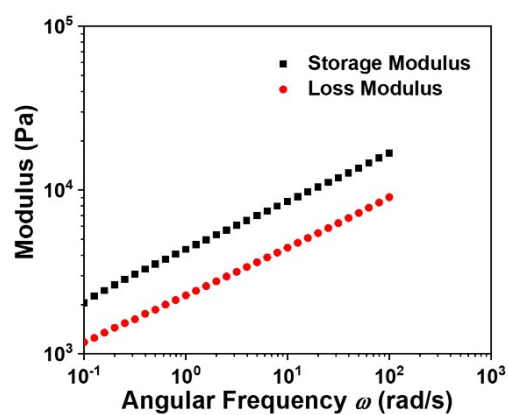


Figure S5. Storage and loss moduli of the ion gel from sample 78-16-6.

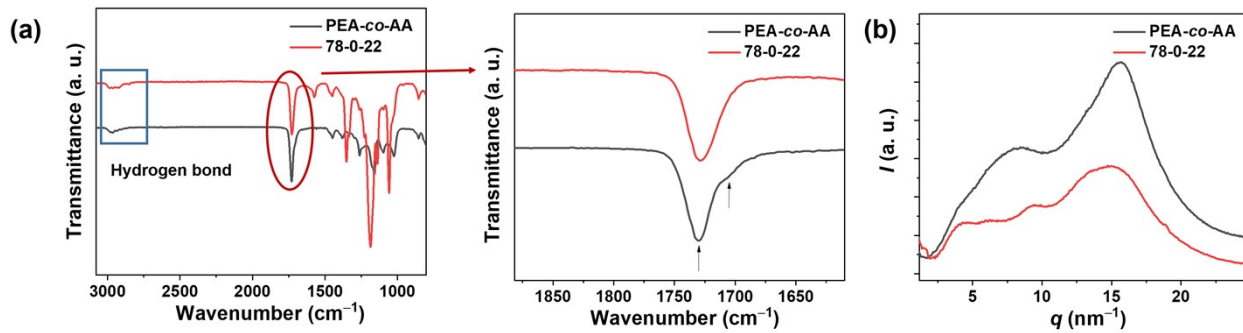


Figure S6. FTIR (a) and WAXS (b) results of PEA-*co*-AA and 78-0-22.

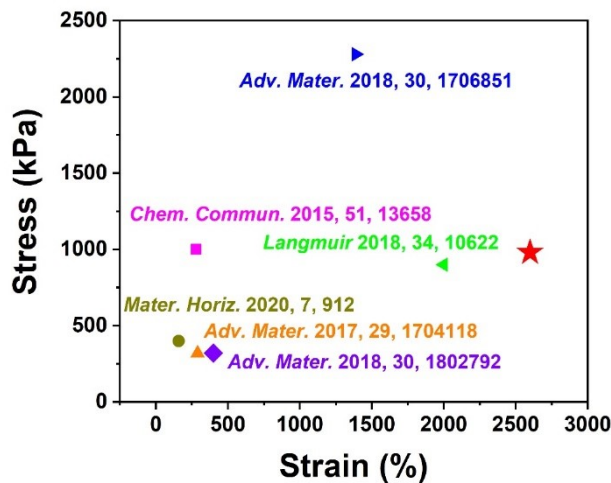


Figure S7. Breaking elongation and failure tensile stress of high-performance ion gels reported in recent years.¹⁻⁶ The red star indicates ion gel from sample 78-10-12 in this work.

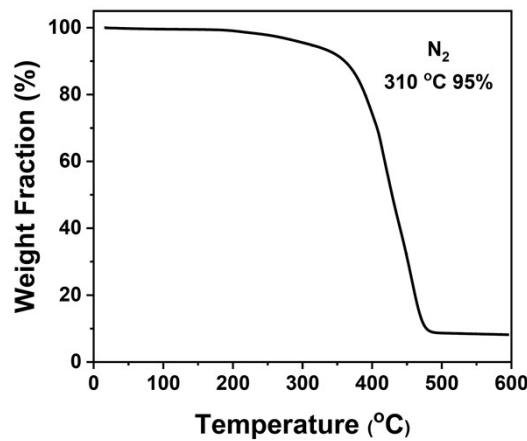


Figure S8. Thermogravimetric curve of the P(EA-*co*-AA-*co*-AANa) ion gel (78-10-12) at a heating rate of $10\text{ }^\circ\text{C min}^{-1}$ under nitrogen.

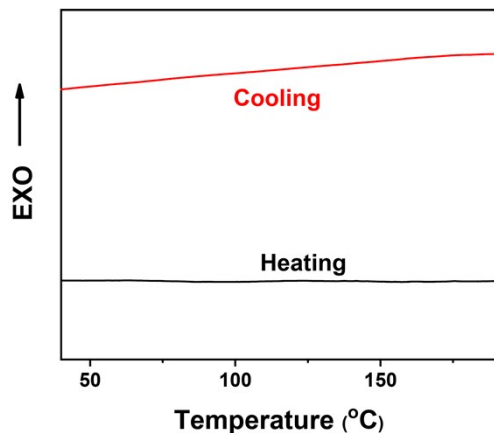


Figure S9. DSC thermogram of the P(EA-*co*-AA-*co*-AANa) ion gel at a heating and cooling rate of $20\text{ }^{\circ}\text{C min}^{-1}$ under a nitrogen atmosphere.

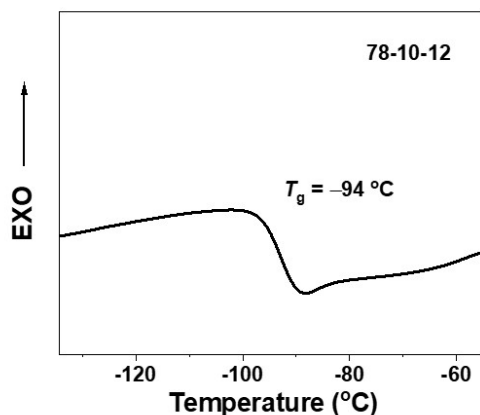


Figure S10. DSC thermogram of the ion gel from sample 78-10-12 at a heating and cooling rate of $20\text{ }^{\circ}\text{C min}^{-1}$ under a nitrogen atmosphere.

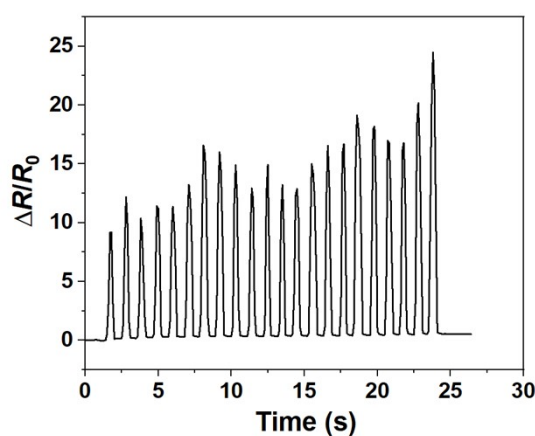


Figure S11. Sensing performance of the strain sensor in large strains.

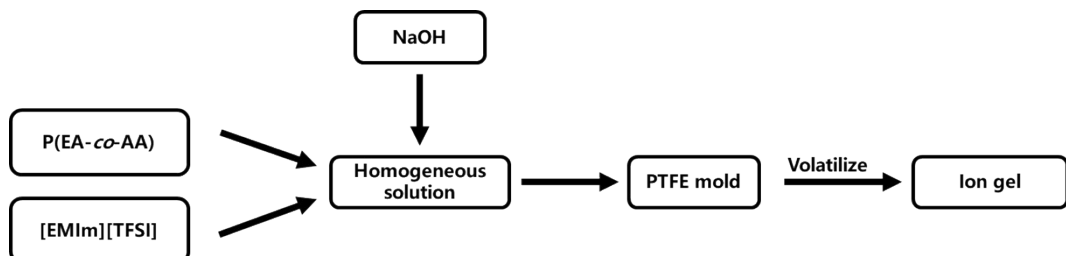


Figure S12. Schematic illustration of the preparation of the P(EA-*co*-AA-*co*-AANa) ion gel.

References

1. M. L. Jin, S. Park, J. S. Kim, S. H. Kwon, S. Zhang, M. S. Yoo, S. Jang, H. J. Koh, S. Y. Cho, S. Y. Kim, C. W. Ahn, K. Cho, S. G. Lee, D. H. Kim and H. T. Jung, *Adv. Mater.*, 2018, **30**, e1706851.
2. F. Moghadam, E. Kamio, A. Yoshizumi and H. Matsuyama, *Chem. Commun.*, 2015, **51**, 13658-13661.
3. T. Yasui, E. Kamio and H. Matsuyama, *Langmuir*, 2018, **34**, 10622-10633.
4. Z. Cao, H. Liu and L. Jiang, *Mater. Horiz.*, 2020, **7**, 912-918.
5. E. Kamio, T. Yasui, Y. Iida, J. P. Gong and H. Matsuyama, *Adv. Mater.*, 2017, **29**, 1704118.
6. R. Tamate, K. Hashimoto, T. Horii, M. Hirasawa, X. Li, M. Shibayama and M. Watanabe, *Adv. Mater.*, 2018, **30**, e1802792.